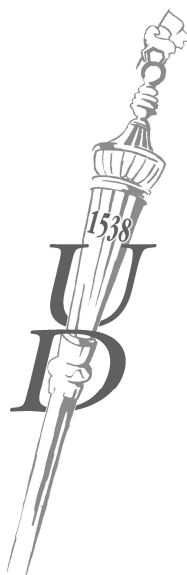


PhD Theses

**PHOTOCHEMICAL AND REDOX
PROPERTIES OF
1,4-BENZOQUINONES**

Éva Józsa

Supervisor: Dr. Katalin Ósz



UNIVERSITY OF DEBRECEN
PhD Program in Chemistry
Debrecen, 2014

I. INTRODUCTION AND OBJECTIVES

Solar energy can be converted to electricity by photovoltaic cells or to thermal energy by solar collectors. Many organisms, such as plants, perform photosynthesis producing high energy compounds, e.g. carbohydrates, and they have a continuous energy supply in this way. There have been many attempts to mimic natural photosynthesis and convert solar energy into fuels starting from the 1970's¹. Such systems could be used theoretically to store solar energy by producing a reasonable quantity of H₂ or other small molecule fuels.

Photosystems that have a band gap larger than 3 eV (semiconductors or organometallic compounds) only use the UV range of the solar spectrum. The efficiency of these systems is questionable. Artificial photosynthetic cells can use two photosystems similarly to the Z-scheme of their natural counterparts. Since the band gap can be much lower (1-2 eV) in such systems their effective spectra is extended to the visible range while still being able to perform water splitting. Water splitting requires 2-3 eV of energy that includes the activation and kinetic overpotential². A good example of shuttle mediators is the plastoquinone-plastoquinol redox couple in naturally occurring photosynthetic electron transports. However, a comparative study on benzoquinone derivatives as possible redox mediators in such systems is lacking.

It was recently demonstrated that the photoreaction of 2,6-dichloro-1,4-benzoquinone produced O₂ and dichloro-hydroquinone. This finding raises the possibility to use direct photoreduction of quinones in artificial photosynthetic systems.

Redox mediators in solar energy conversion systems must fulfil a set of criteria including low overpotential in electrode reactions, fast electron

transfer rate, fast diffusion, photoresistance and insensitivity to reactive oxygen species. Characterization of potential redox mediators thus must include the assessment of their electrochemical and photochemical properties.

Our aim was to study the photoreactions of different 1,4-benzoquinone derivatives having electron withdrawing or electron donating substituent(s) with spectrophotometric and pH-stat methods, spectrofluorimetric approaches, and using a photoreactor designed by our research group.

It was among our goals to develop a simplified actinometric method in order to assess the photon flux of light sources used in our study.

We aimed to investigate the electrochemical properties of different quinone/quinol redox systems.

In order to understand the effect of oxidizing compounds formed by excitation of 1,4-benzoquinones and of reactive oxygen species that may form in artificial photosystems, we aimed to conduct kinetic studies on the 1,4-benzoquinones – H₂O₂ reactions.

LIST OF ABBREVIATIONS

Q: 1,4-benzoquinone; **Q-H₂**: 1,4-hydroquinone; **Q-OH**: 2-hydroxy-1,4-benzoquinone; **QMe**: 2-methyl-1,4-benzoquinone; **QMe-H₂**: 2-methyl-1,4-hydroquinone; **QMe-OH**: 2-methyl-5-hydroxy-1,4-benzoquinone; **QMe₂**: 2,6-dimethyl-1,4-benzoquinone; **Q(MeO)₂**: 2,6-dimethoxy-1,4-benzoquinone; **Q(MeO)₂-H₂**: 2,6-dimethoxy-1,4-hydroquinone; **QMe(MeO)₂**: 2,3-dimethoxy-5-methyl-1,4-benzoquinone; **QMe(MeO)₂-H₂**: 2,3-dimethoxy-5-methyl-1,4-hydroquinone; **Q-2,5-Cl₂**: 2,5-dichloro-1,4-benzoquinone; **Q-2,5-Cl₂-OH**: 2,5-dichloro-3-hydroxy-1,4-benzoquinone; **Q-2,6-Cl₂**: 2,6-dichloro-1,4-benzoquinone; **Q-2,6-Cl₂-OH**: 2,6-dichloro-3-hydroxy-1,4-benzoquinone; **QR**: quinones having -R functional group; **QR-H₂**: 1,4-hydroquinones having -R functional group; **QR-OH**: hydroxy-1,4-benzoquinones having -R functional group;

Equations (8) and (9): **q_p**: photon flux; **N_A**: Avogadro constant; **V**: volume of the illuminated solution; **Φ₃₆₅**: differential quantum yield of the actinometer at wavelength 365 nm; **ε₃₉₀**: molar absorption coefficient for the actinometer at wavelength 390 nm; **l**: optical path length; **c_{Fe(II)}**: Fe(II) concentration; **C**: ratio of the actual and relative energies for the instrument ($C = E_{\lambda} / E_{\lambda}^{rel}$); **h**: Planck constant; **c**: speed of light

Equations (10) and (11): **c₀**: initial concentration of the reactant; **A_λⁱⁿⁱ** and **A_λ^{fin}**: initial and final absorbances detected at the wavelength of the detection, **A_Φⁱⁿⁱ** and **A_Φ^{fin}**: initial and final absorbances measured at the illumination wavelength, **β**: ratio of the path length of illumination and detection, **ξ**: kinetic reaction coordinate

II. EXPERIMENTAL METHODS

Aqueous solutions of 1,4-benzoquinone derivatives were prepared using triply ion exchanged (Millipore) water.

Kinetic studies of the formation and the decomposition of hydroxy quinones were performed by UV-Vis spectrophotometry. A Shimadzu UV-1601 double beam spectrophotometer with UV-Probe software was used for measuring the spectrum of the hydroxyquinone product. Only one wavelength at the maximum absorbance in the visible range was used to follow the reaction. For the oxidation reactions of Q at higher hydrogen peroxide concentrations (0.09-0.18 mol dm⁻³), rapid kinetic experiments were carried out in an Applied Photophysics DX-17 MV stopped-flow instrument with photomultiplier tube as the detector.

Kinetic studies of the photochemical reaction of QR derivatives were carried out by an AnalytikJena SPECORD S600 diode array spectrophotometer and ABU 91 AUTOBURETTA RADIOMETER COPENHAGEN pH stat instrument equipped with a UV lamp. Moreover, this type of reactions were performed by a photochemical reactor combining an Avantes Avaspec-2048 CCD spectrophotometer and a LED radiation source.

Spectrophotometric titrations were carried out for the determination of the pK_a values of the QR-OH. They were produced during the photochemical reaction with a Spectroline FC-100/F UV-A lamp emitting at 365 nm in a thermostatted sample holder. Carbonate free argonated KOH solution was used during pH stat measurements.

Spectrofluorimetry was used to analyze the fluorescence emission spectra of Q-H₂ and QMe-H₂ and to follow the formation of Q-H₂ during

the photoreaction of Q. The fluorescence spectra were recorded with a Jasco FP-8500 fluorimeter.

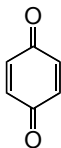
The least squares fitting of the measured data during spectrophotometric titration and kinetic experiments was carried out using the general fitting software MicroMath SCIENTIST.

To identify the decomposition products of QMe-OH, $^1\text{H-NMR}$ spectroscopy and GC-MS measurements were carried out. $^1\text{H-NMR}$ spectra were measured on a BRUKER DRX 400 instrument. For the evaluation of the spectra, the MestReNova NMR software was used. GC-MS measurements were carried out using a Shimadzu GCMS-QP2010plus system and the compounds were identified by using NIST05 library spectra.

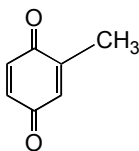
Cyclic voltammetric measurements were performed to determine the formal potential values of the quinone/hydroquinone redox systems, the $\text{p}K_{\text{a}1}$ values of Q-H₂, QMe(MeO)₂-H₂, QCl-H₂, and heterogeneous electron transfer rate constant of Q-H₂ and QMe(MeO)₂-H₂ on platinum electrode. During the experiments, platinum was used as the working electrode and counter electrode, while the reference electrode was an Ag/AgCl electrode. The cyclic voltammograms were obtained by means of a Metrohm VA 746 Trace Analyzer equipped with 747 VA Stand. For the analysis of the voltammograms, the CACYVO program was used.

For the pH measurements of the benzoquinone solutions, a Metrohm hydrogenion selective glass electrode connected to an ABU 93 Triburette potentiometric titrator or mobile pH meter was used.

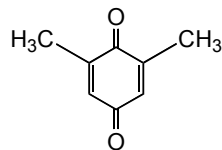
STRUCTURAL FORMULA OF THE STUDIED 1,4-BENZOQUINONE
DERIVATIVES



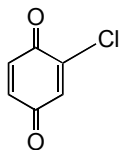
1,4-benzoquinone



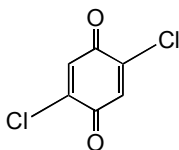
2-methyl-
1,4-benzoquinone



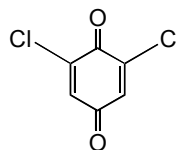
2,6-dimethyl-
1,4-benzoquinone



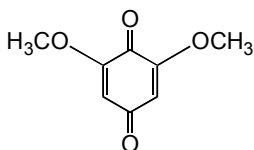
2-chloro-
1,4-benzoquinone



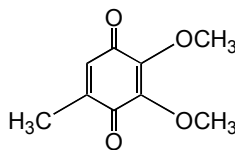
2,5-dichloro-
1,4-benzoquinone



2,6-dichloro-
1,4-benzoquinone



2,6-dimethoxy-
1,4-benzoquinone



2,3-dimethoxy-5-methyl-
1,4-benzoquinone

III. SCIENTIFIC ACHIEVEMENTS

1. We determined the kinetic properties of H_2O_2 oxidation of Q, QMe and QCl.

The formation and decomposition of the reaction was monitored at the wavelength of absorbance maximum of QR-OH in the visible range (Figure 1). The high excess of H_2O_2 assured the constant concentration of the oxidizing agent. The pH of the solution was maintained at constant values using phosphate buffer in excess. The kinetic traces were fitted based on the kinetic scheme expressed with equations (1) and (2).

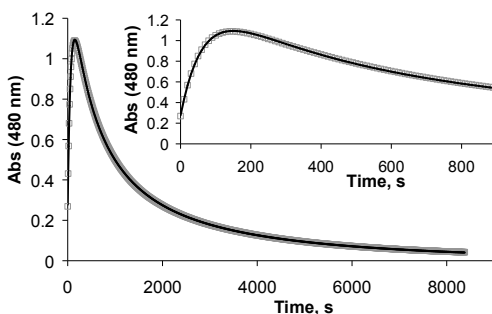
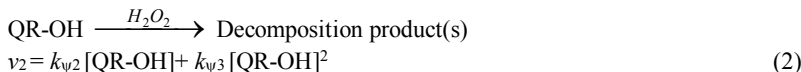


Figure 1:

Kinetic trace during the reaction $Q-H_2O_2$ at 25.0 °C; $c(Q) = 8.7 \times 10^{-4} \text{ mol dm}^{-3}$; $c(H_2O_2) = 0.54 \text{ mol dm}^{-3}$; pH = 6.52; \square : experimental data; — : fitted curve



The fitted parameters were the molar absorption of QR-O⁻, and the apparent rate constants $k_{\psi 1}$, $k_{\psi 2}$ and $k_{\psi 3}$.

Based on our results, the formation of QR-OH can be expressed as follows:

$$v_1 = k_{\psi 1}[\text{QR}] = k_1 \frac{[\text{QR}][\text{H}_2\text{O}_2]}{[\text{H}^+]} \quad (3)$$

The rate limiting step was the reaction of QR with the deprotonated form of H₂O₂ (HO₂⁻) which was preceded by the fast pre-equilibrium of H₂O₂ deprotonation.



The rate constants (k_1), the molar absorbances of QR-O⁻, and the pK_a values of QR-OH based on spectrophotometric titration are listed in Table 1.

Table 1: The k_1 values of the formation of QR-OH, pK_a values of QR-OH and molar absorbance (ϵ) of its deprotonated form at 25.0 °C; *: literature data

Quinone derivative	k_1, s^{-1}	pK _a (QR-OH)	ϵ (QR-O ⁻), dm ³ mol ⁻¹ cm ⁻¹
QMe	$(3.46 \pm 0.01) \times 10^{-9}$	4.5 ± 0.4	817 ± 20 (490 nm)
Q	$(1.23 \pm 0.02) \times 10^{-8}$	3.4 ± 0.1	1703 ± 88 (480 nm)
QCl	$(1.49 \pm 0.03) \times 10^{-7}$	2.8 ± 0.6	823 ± 10 (510 nm)
Q-2,6-Cl ₂	2.7×10^{-7} *	1.8 ± 0.6	2530 ± 60 (524 nm) *

The ¹H-NMR measurements of the reaction products suggest that QMe-OH decomposes to aliphatic fragments.

2. We calculated the activation parameters of the rate limiting step of H_2O_2 oxidation of Q, QMe, QCl and Q-2,6-Cl₂.

Temperature dependent experiments were carried out at in the temperature range between 10-40 °C (Figure 2). The rate constant (k_b) of the rate limiting process of Q, QMe, QCl, Q-2,6-Cl₂ oxidation with H_2O_2 was calculated from the fitted $k_{\psi 1}$ and the temperature dependent K_a values of H_2O_2 (6, 7).

$$k_1 = k_{\psi 1} \frac{[H^+]}{[H_2O_2]} \quad \text{and} \quad k_b = \frac{k_1}{K_{s,H_2O_2}} \quad (6, 7)$$

This k_b value was used to express the activation energy, activation enthalpy, and activation entropy (E_a , ΔH^\ddagger , and ΔS^\ddagger , respectively) from the Eyring and Arrhenius plots (Table 2).

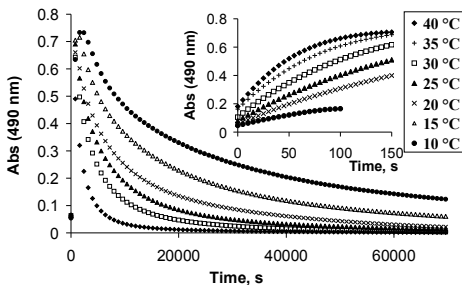


Figure 2:

Kinetic curves measured at different temperatures for the reaction QMe- H_2O_2 ; $c(QMe) = 9.5 \times 10^{-4} \text{ mol dm}^{-3}$, $c(H_2O_2) = 0.58 \text{ mol dm}^{-3}$, $pH = 6.39$

Table 2: Activation parameters of the rate limiting step for the formation of QR-OH

Quinone derivative	E_a , kJ mol ⁻¹	ΔH^\ddagger , kJ mol ⁻¹	ΔS^\ddagger , J mol ⁻¹ K ⁻¹
QMe	18.4±0.4	15.9±0.4	-129±1
Q	15.3±1.3	12.9±1.3	-127±4
QCl	8.9±0.6	6.5±0.6	-128±2
Q-2,6-Cl ₂	5.5±0.3	3.0±0.3	-142±1

3. We developed a simplified actinometric measurement method to assess the photon flux of light sources.

The ferrioxalate actinometric method recommended by the IUPAC guidelines was simplified. We omitted the addition of coordination ligand after completing the actinometric reaction and instead of that, we measured directly the spectral changes that follow the photoreduction of Fe(III) to Fe(II) in the UV range by spectrophotometry (Figure 3).

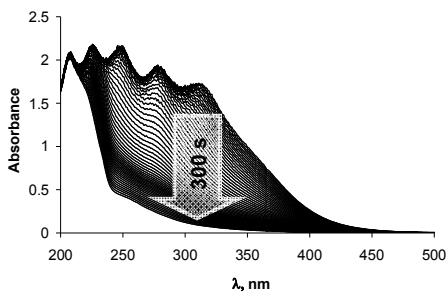


Figure 3:
Spectral changes of the actinometer during 5-min illumination by the UV lamp;
 $c\{\text{K}_3[\text{Fe}(\text{C}_2\text{O}_4)_3] \cdot 3\text{H}_2\text{O}\} = 1.17 \times 10^{-3} \text{ mol dm}^{-3}$

We analyzed the photon flux of the light sources of the diode array spectrophotometer in parallel measurements and we found that the relative error of the new method is significantly lower (6%) than that of classical actinometry (9%). The new method is based on continuous monitoring of the actinometric reaction process thus it enables stability measurements of the light sources. In the case of monochromatic light, equation (8) can be used to calculate the photon flux that enters a given reaction volume, while in case of polychromatic light, equation (9) was used to compute a photon flux spectrum (symbols are listed in the abbreviation part).

$$q_p = \left(\frac{dA_{390}}{dt} \right) \frac{N_A V}{\Phi_{365} \epsilon_{390} l} \quad (8)$$

$$v = \frac{dc_{\text{Fe(II)}}}{dt} = C \int \frac{\Phi_{\lambda} E_{\lambda}^{\text{rel}} \lambda}{N_A hc V t} (1 - 10^{-A_{\lambda}}) d\lambda \quad (9)$$

4. We constructed a special photochemical reactor combining a fiber-optic spectrophotometer for monitoring the photodecomposition of 1,4-benzoquinone derivatives.

In order to study photoreactions in a controlled geometry setup, we designed and built a photoreactor. The reactor consists of a holder compatible with a 12.5×12.5×45 mm quartz cuvette that can be irradiated from the top using a LED light source (Figure 4). The boreholes on the opposite sides of the housing support the collimating lenses and the fiber optics of the spectrophotometer used to follow the reaction process. The fiber optics connects the detector and the light source of the photometer to the reactor. As the photon flux of the spectrophotometer is insufficient to drive the photoreaction, it does not interfere with the LED induced reaction. Thorough stirring of the sample must be assured during the whole photochemical process. The cell holder is made out of brass thus enabling magnetic stirring. The LED light sources are controlled by a personal computer, thus different intensities and irradiation time profiles can be set.

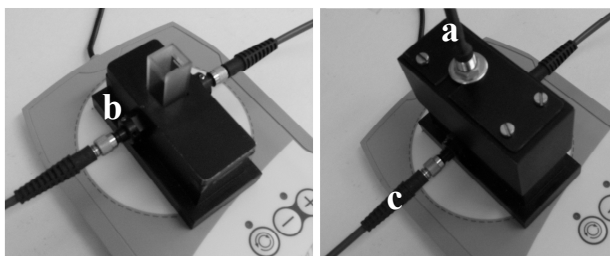


Figure 4: Cell holder of the photoreactor; a: LED light source; b: collimating lenses; c: optical fiber

5. We determined the quantum yield for the photodecomposition of Q, QCl, Q-2,5-Cl₂ and Q-2,6-Cl₂ induced by a LED₄₀₀.

The process of the photoreaction of QCl, Q-2,5-Cl₂ and Q-2,6-Cl₂ was followed in unbuffered solution at the absorption maximum wavelength of the deprotonated form of their hydroxy derivative. In the case of Q, the pH in unbuffered aqueous solution is similar to the pK_a of Q-OH, thus the kinetic trace at the isobestic wavelength of the Q-OH and Q-O⁻ + H⁺ process was used to determine the quantum yield (Table 3). The fitted model was based on equations (10) and (11) (symbols are listed in the abbreviation part).

$$\frac{d\zeta}{dt} = \frac{q_{n,p}\Phi}{Vc_0} \left(1 - 10^{-(1-\zeta)\beta A_{\Phi}^{ini} - \zeta\beta A_{\Phi}^{fin}} \right) \frac{(1-\zeta)A_{\Phi}^{ini}}{(1-\zeta)A_{\Phi}^{ini} + \zeta A_{\Phi}^{fin}} \quad (10)$$

$$A_{\lambda} = (1-\zeta)A_{\lambda}^{ini} + \zeta A_{\lambda}^{fin} \quad (11)$$

Table 3: Quantum yield for the decomposition of QR and parameters derived from fitting and used for curve fitting; $T = 25.0\text{ }^{\circ}\text{C}$

	Q	QCl	Q-2,5-Cl ₂	Q-2,6-Cl ₂
Φ_{400}	0.34	1.11	1.34	1.10
$q_{n,p}\Phi(Vc_0)^{-1}, \text{ s}^{-1}$	$(1.76 \pm 0.05) \times 10^{-3}$	$(5.70 \pm 0.09) \times 10^{-3}$	$(2.08 \pm 0.02) \times 10^{-3}$	$(5.65 \pm 0.05) \times 10^{-3}$
A_{λ}^{ini}	0.0444 (425 nm)	0.0275 (510 nm)	0.145 (524 nm)	0.0161 (524 nm)
A_{λ}^{fin}	0.386 (425 nm)	0.815 (510 nm)	0.908 (524 nm)	0.848 (524 nm)
A_{Φ}^{ini} (400 nm)	0.0300	0.0579	0.184	0.110
A_{Φ}^{fin} (400 nm)	0.505	0.297	0.351	0.167
$q_p, \text{ s}^{-1}$	7.7×10^{15}	7.7×10^{15}	2.8×10^{15}	7.7×10^{15}
β	2.5			

6. We monitored the formation of *Q-OH* and *Q-2,6-Cl₂-OH* selectively based on their spectral and acid-base characteristics.

The photoreactions were induced by a UV lamp and the reaction process was followed by spectrophotometry and pH-stat titration. The quantum yield of QR-OH formation at 365 nm wavelength was determined using the initial rate method (Equation 12). The kinetic traces were evaluated using the molar absorbance of QR-O⁻ (Table 1).

The results of pH-stat titration measurements of photoreactions did not show a significant difference from those obtained by spectrophotometry (Table 4). These results show that H⁺ formation is attributable solely to deprotonation of QR-OH, thus the amount of base consumed during the pH-stat measurement reflects the concentration of QR-OH.

$$v_{ini} = \frac{\Phi q_p}{V} \left(1 - 10^{-\beta A_{\Phi}^{ini}} \right) \quad (12)$$

Table 4: Initial rate and quantum yield for the formation of QR-OH and the initial absorbances measured at the wavelength of the illumination; $T = 25.0$ °C

Quinone derivative		Q	Q-2,6-Cl ₂
Spectrophotometric method $\beta=2.5$	Φ_{365}	0.07	0.40
	v_{ini} , mol dm ⁻³ s ⁻¹	6.75×10^{-8}	2.28×10^{-6}
	q_p , s ⁻¹	9.54×10^{15}	9.54×10^{15}
pH-stat method $\text{pH} \approx \text{p}K_{a(\text{QR-OH})} + 2$ $\beta=1.77$	Φ_{365}	0.08	0.47
	v_{ini} , mol dm ⁻³ s ⁻¹	8.05×10^{-8}	3.39×10^{-6}
	q_p , s ⁻¹	2.7×10^{17}	2.7×10^{17}
A_{Φ}^{ini} (365 nm)		0.029	0.39

7. We measured the fluorescence spectral characteristics of $Q-H_2$ and $QMe-H_2$.

Both $Q-H_2$ and $QMe-H_2$ show an excitation maximum at 290 nm and a fluorescence emission peak at 330 nm in aqueous solution. The fluorescence emission was used to follow $QR-H_2$ formation during the photoreaction of QR. However, the absorption spectra of QMe and Q

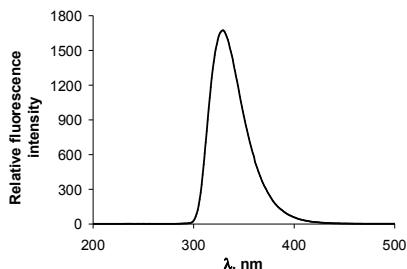


Figure 5: Fluorescence emission spectrum of $QMe-H_2$; $\lambda_{ex} = 290$ nm

overlap with the fluorescent emission of its $QR-H_2$, causing a strong internal filter effect. To assess the extent of this effect we measured mixtures of QMe and $QMe-H_2$ in different ratios. We found that in samples diluted to 5×10^{-5} mol dm^{-3} ($[QR-H_2] + [QR]$), the inner filter effect was diminished and the fluorescence emission showed linear correlation with the $QR-H_2$ concentration regardless of the QR fraction in the solution (Figure 6). Irradiating such dilute QR solutions would result in very slow reaction progress. Irradiating samples of 1×10^{-3} mol dm^{-3} Q , then diluting them $20 \times$ before fluorimetry, we assessed the quantum yield of $Q-H_2$ formation: 0.21.

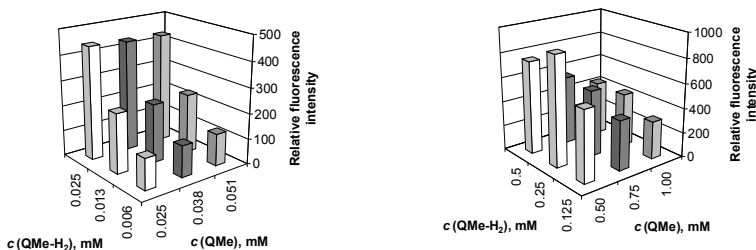


Figure 6: Analysis the correlation between $c(QMe-H_2)$ and the fluorescence intensity in the presence of QMe

8. We determined the dependence of formal potential of $Q/Q-H_2$, $QMe/QMe-H_2$, $Q(MeO)_2/Q(MeO)_2-H_2$, $QMe(MeO)_2/QMe(MeO)_2-H_2$, $QCl/QCl-H_2$, $Q-2,6-Cl_2/Q-2,6-Cl_2-H_2$ from the nature of substituents and assessed the pK_{a1} in case of $Q-H_2$, $QMe(MeO)_2-H_2$ and $QCl-H_2$.

The pH independent parts of Pourbaix diagrams derived from cyclic voltammetric measurements of unbuffered solutions of QR were compared (Figure 7). We found that the higher the electropositivity of substituents the lower the formal potential of that given QR/QR- H_2 was.

We determined the pK_{a1} values of $Q-H_2$, $QMe(MeO)_2-H_2$ and $QCl-H_2$ by measuring the pH dependence of their formal potential values in buffered solutions (9.7; 11.3; 8.2, respectively). We found that the minimum of the peak separations is in agreement with pK_{a1} values. The pK_{a1} values are also in linear correlation with the formal potentials of QR/QR- H_2 redox systems (Figure 8). A similar correlation was published for the semiquinone/quinone systems.

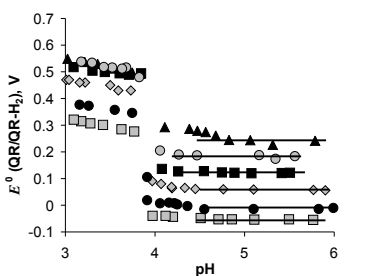


Figure 7: Pourbaix diagrams of QR/QR- H_2 redox systems; $T = 25.0\text{ }^\circ\text{C}$;
 ▲: Q-2,6- Cl_2 ; ●: QCl; ■: Q; ◆: QMe; ●: QMe(MeO) $_2$; ■: Q(MeO) $_2$

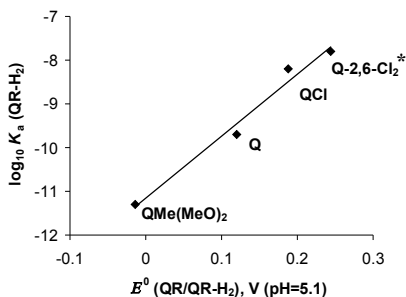


Figure 8: The $\log_{10} K_a$ values of QR- H_2 as a function of E^0 for QR/QR- H_2 ; $T = 25.0\text{ }^\circ\text{C}$; *: $\log_{10} K_a$ from literature

9. We assessed the diffusion constant and the heterogeneous electron transfer rate constant of Q-H₂ and QMe(MeO)₂-H₂ on platinum electrode.

The cyclic voltammograms of Q/Q-H₂, and QMe(MeO)₂/QMe(MeO)₂-H₂ redox systems were studied at different sweeping rates. The diffusion constants were derived from the diffusion controlled part of the E_p -lg ν function for Q-H₂ and QMe(MeO)₂-H₂ based on the Randles-Sevcik method (Figure 9).

The heterogeneous electron transfer rate constants on the Pt electrode were also determined using the peak potential depending part on the sweeping rate of this function, according to Nicholson and Shain (Table 5).

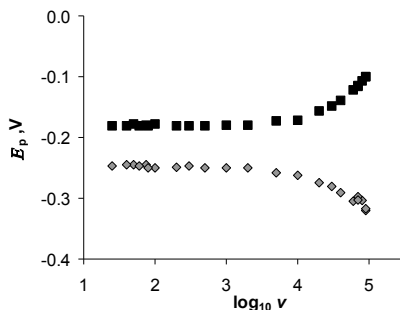


Figure 9: Peak potentials of QMe(MeO)₂/QMe(MeO)₂-H₂ redox system (E_p) as a function of \log_{10} of scan rate (ν , mV s⁻¹); $T = 25.0$ °C

Table 5: Diffusion coefficients and heterogeneous electron transfer rate constant for QR/QR-H₂ at 25.0 °C

Quinone derivative	D , cm ² s ⁻¹	k_s , cm s ⁻¹
Q/Q-H ₂	1.63×10^{-6}	0.031
QMe(MeO) ₂ /QMe(MeO) ₂ -H ₂	2.02×10^{-6}	0.035

10. We found a linear correlation between the k_1 of $QR - H_2O_2$ reactions, the activation energy for the rate determining step of this reaction, the formal potential of $QR/QR-H_2$ redox systems and the pK_a values of $QR-OH$.

We found that the electron withdrawing or electron donating property of different substituents influenced the rate and the activation energy of $QR - H_2O_2$ reaction significantly, the formal potential of $QR/QR-H_2$ redox systems and the pK_a of $QR-OH$. These values correlate to each other upon different substituents, which suggests that these values are determined by common structural background and can be shifted as a function of the substituents electronegativity (Figures 10 and 11).

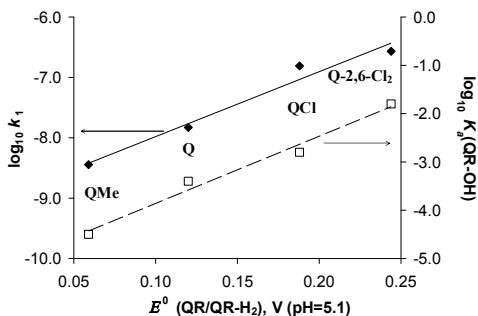


Figure 10: Linear correlation between $\log_{10} k_1$ values for $QR-H_2O_2$ reactions (y-axis, \blacklozenge); $\log_{10} K_s$ values of $QR-OH$ (y-axis, \square) and formal redox potential of the $QR/QR-H_2$ systems (x-axis); $T = 25.0\text{ }^\circ\text{C}$

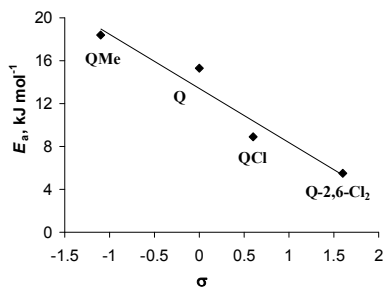


Figure 11: Linear correlation between activation energy for the rate limiting step of $QR - H_2O_2$ reaction and the Hammett-like substituent constants (σ) derived from pK_a values of $QR-OH$; $T = 25.0\text{ }^\circ\text{C}$

IV. POSSIBLE APPLICATIONS OF THE RESULTS

Our studies revealed that photoreactions of photosensitive QR lead to the formation of QR-OH. The quantum yields of the QR-OH and QR-H₂ varied between different R substituted derivatives. These results show that photosensitive quinones (Q, QMe, QCl, Q-2,5-Cl₂, Q-2,6-Cl₂) cannot be used for solar energy conversion.

The photosensitivity of Q(MeO)₂ and QMe(MeO)₂ is minor, their photoreaction is far from being efficient.

In natural photosynthetic systems, plastoquinone, a 1,4-benzoquinone derivative, is one of the most important mediators between the two photosystems. One form of artificial photosynthetic cells following the Z-scheme uses soluble redox mediators between semiconductor based photosystems (O₂ and H₂ evolving systems) to connect the electrochemical chain.

Our results show that non-photosensitive quinones like QMe(MeO)₂ may be used in artificial photosynthetic systems as redox mediators (Figure 12). The Q(MeO)₂-H₂ or QMe(MeO)₂-H₂ oxidation and H⁺ reduction together has a substantially lower energy requirement than complete water splitting (the gap between the redox potentials of QR/QR-H₂ and H⁺/H₂ redox systems). Thus combining solar irradiation with electrolysis could be an efficient way to produce H₂ (Figure 13). On platinum electrodes, the overpotential of H₂ generation is only 0.07 volts. The oxidation and reduction overpotential of Q(MeO)₂ and QMe(MeO)₂ is low at neutral and basic unbuffered solution, and higher at acidic condition that lower the efficiency of reoxidation.

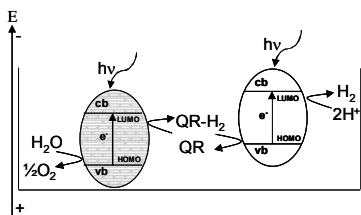


Figure 12: Artificial photosynthetic system containing quinone mediator based on the Z-scheme

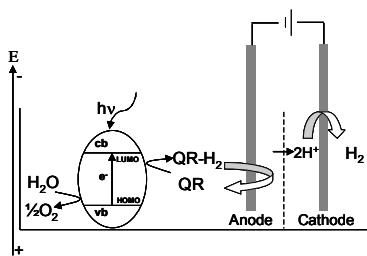


Figure 13: Light assisted electrolytic cell for water splitting containing quinone as mediator

V. LIST OF PUBLICATIONS

Papers related to the dissertation:

1. Éva Józsa, Mihály Purgel, Marianna Bihari, Péter Pál Fehér, Gábor Sustyák, Balázs Várnagy, Virág Kiss, Eszter Ladó and Katalin Ósz
Kinetic studies of hydroxyquinone formation from water soluble benzoquinones

New Journal of Chemistry, **2014**, 38, 588

IF: 2,966 (2012)

2. Tímea Lehóczki, Éva Józsa, Katalin Ósz

Ferrioxalate actinometry with online spectrophotometric detection

Journal of Photochemistry and Photobiology A - Chemistry, **2013**, 251, 63.

IF: 2,416 (2012)

3. Melinda Gombár, Éva Józsa, Mihály Braun and Katalin Ósz

Construction of a photochemical reactor combining a CCD spectrophotometer and a LED radiation source

Photochemical and Photobiological Sciences, **2012**, 11, 1592

IF: 2,923

Other publication:

4. Éva Józsa, Katalin Ósz, Csilla Kállay, Paolo de Bona, Chiara A. Damante, Giuseppe Pappalardo, Enrico Rizzarelli, and Imre Sóvágó
Nickel(II) and mixed metal complexes of amyloid- β N-terminus. Results of potentiometric and spectroscopic studies on the binary nickel(II) and mixed metal nickel(II)-copper(II) and nickel(II)-copper(II)-zinc(II) complexes of peptide fragments

Dalton Transactions, **2010**, 39, 7046

IF: 3,647

Lectures and posters related to the dissertation:

Lectures:

1. Józsa Éva*, Ósz Katalin

1,4-Benzokinin-származékok fotokémiai és redoxisajátságai

MTA Reakciókinetikai és Fotokémiai Munkabizottságának ülése

2014. május 26-27., Siófok, Magyarország

2. Kiss Virág*, Józsa Éva, Ósz Katalin

1,4-Benzokininok redukciójának kinetikai vizsgálata

MTA Reakciókinetikai és Fotokémiai Munkabizottságának ülése

2014. május 26-27., Siófok, Magyarország

3. Józsa Éva

A fényenergia hasznosításának lehetőségei – Kinonok foto- és elektrokémiai reakciói

Debreceni Egyetem, Fizikai Kémiai Tanszék szeminárium-sorozata, Nemzeti Kiválóság Program, Apáczai Csere János Doktoranduszi Ösztöndíj teljesítés

2014. február 26., Debrecen, Magyarország

4. Józsa Éva, Ósz Katalin*, Purgel Mihály

Vizoldható benzokininok oxidációs reakcióinak kinetikai vizsgálata

Magyar Tudományos Akadémia Reakciókinetikai és Fotokémiai Munkabizottságának ülése

2013. szeptember 26-27., Mátraháza, Magyarország

5. Józsa Éva

A fényenergia hasznosításának lehetősége 1,4-benzokinin származékokkal

XXXVI. Kémiai Előadói Napok

2013. október 28-30., Szeged, Magyarország

6. Józsa Éva*, Beyer Dániel Ernő, Ósz Katalin

A fényenergia hasznosításának lehetőségei

Debreceni Egyetem, Fizikai Kémiai Tanszék szeminárium-sorozata, Nemzeti Kiválóság Program, Apáczai Csere János Doktoranduszi Ösztöndíj teljesítés

2013. június 6., Debrecen, Magyarország

7. Józsa Éva, Ósz Katalin*, Szatmári Enikő, Bradács Orsolya

Szubsztituált *para*-benzokininok fotoreakciója fémionok jelenlétében

47. Komplexkémiai Kollokvium

2013. május 29-31., Mátraháza, Magyarország

8. Józsa Éva*, Ósz Katalin

A fényenergia hasznosításának lehetősége 1,4-benzokinin származékokkal

Magyar Tudományos Akadémia Reakciókinetikai és Fotokémiai Munkabizottságának ülése

2013. április 25-26., Siófok, Magyarország

9. Józsa Éva*, Kiss Virág, Ósz Katalin

Kinonok fotokémiai reakcióinak vizsgálata

Magyar Tudományos Akadémia Reakciókinetikai és Fotokémiai Munkabizottságának ülése

2012. október 25-26., Gyöngyöstarján, Magyarország

10. Katalin Ósz*, Éva Józsa, Virág Kiss

Kinetic studies on the photo-oxidation reaction of water by quinones

4th EuCheMS Chemistry Congress

2012. augusztus 26-30., Prága, Csehország

11. Éva Józsa*, Ádám Péter Pap, Virág Kiss, Judit Michnyóczki, Katalin Ósz

Possibilities to utilize solar energy in homogeneous aqueous medium: the use of metal ions and/or quinones as photocatalysts

46. Komplexkémiai Kollokvium

2012. május 21-23., Mátrafüred, Magyarország

12. Józsa Éva*, Ósz Katalin

Szubsztituált kinonok fotokémiai oxidációja vizes közegben

Magyar Tudományos Akadémia Reakciókinetikai és Fotokémiai Munkabizottságának ülése

2011. május 5-6., Siófok, Magyarország

Posters:

1. Éva Józsa*, Katalin Ósz

Photochemical and Oxidation Reactions of Water Soluble 1,4-Benzoquinones

European Colloquium on Inorganic Reaction Mechanisms

2014. június 17-20., Debrecen, Magyarország

2. Virág Kiss*, Éva Józsa, Katalin Ósz

Kinetics of the reaction between 2,5-dichloro-1,4-benzoquinone and sulfite ion

European Colloquium on Inorganic Reaction Mechanisms

2014. június 17-20., Debrecen, Magyarország

3. Éva Józsa*, Virág Kiss, Marianna Bihari, Enikő Szatmári, Orsolya Bradács, Katalin Ósz
Photochemical reactions of 1,4-benzoquinones in homogeneous aqueous medium
8th International Conference on Chemical Kinetics
2013. július 8-12., Seville, Spanyolország
4. Éva Józsa*, Eszter Ladó, Dániel Ernő Beyer, Katalin Ósz
pH dependent formal potentials of 1,4-benzoquinone derivatives
Debrecen Colloquium on Inorganic Reaction Mechanisms
2013. június 11-15., Debrecen, Magyarország
5. Virág Kiss*, Éva Józsa, Katalin Ósz
Redox and spectrophotometric studies of the photo-decomposition products of quinone derivatives
Debrecen Colloquium on Inorganic Reaction Mechanisms
2013. június 11-15., Debrecen, Magyarország
6. Éva Józsa, Enikő Szatmári*, Orsolya Bradács*, Katalin Ósz
Photochemical reactions of substituted *para*-benzoquinone derivatives in the presence of redox metal ions
Debrecen Colloquium on Inorganic Reaction Mechanisms
2013. június 11-15., Debrecen, Magyarország
7. Ádám Péter Pap, Éva Józsa, Adrienn Vas, Judit Michnyóczki, Katalin Ósz*
Photochemical water splitting catalyzed by cerium(III) complexes
Debrecen Colloquium on Inorganic Reaction Mechanisms
2013. június 11-15., Debrecen, Magyarország
8. Mihály Purgel*, Marianna Bihari, Éva Józsa, Balázs Várnagy, Gábor Sustyák, Katalin Ósz
Kinetics and mechanistic studies of 1,4-benzoquinone and its 2-methyl derivative
Debrecen Colloquium on Inorganic Reaction Mechanisms
2013. június 11-15., Debrecen, Magyarország
9. Éva Józsa*, Virág Kiss, Marianna Bihari, Enikő Szatmári, Orsolya Bradács, Katalin Ósz

Photochemical reaction of 1,4-benzoquinones in homogeneous aqueous medium

Gordon Research Conference, Inorganic Reaction Mechanisms

2013. március 3-8., Galveston, TX, USA

10. Katalin Ósz, Éva Józsa*, Ádám Péter Pap, Judit Michnyóczki

Kinetic studies on the light induced water splitting catalyzed by the Ce(III)/Ce(IV) redox system

International Symposium on Metal Complexes

2012. június 18-22., Lisszabon, Portugália

11. Józsa Éva*, Gombár Melinda, Braun Mihály, Ósz Katalin

Kinonok fotokémiai reakcióinak vizsgálata

Magyar Kémikusok Egyesülete 1. Nemzeti Konferencia

2011. május 22-25., Sopron, Magyarország

12. Melinda Gombár, Éva Józsa, Mihály Braun, Katalin Ósz*

Mechanistic aspects of the photooxidation of water by quinones

Gordon Research Conferences, Inorganic Reaction Mechanisms

2011. március 6-11., Galveston, TX, USA

* person presenting lectures or posters

Köszönetnyilvánítás:

A kutatás a TÁMOP 4.2.4.A/2-11-1-2012-0001 azonosító számú Nemzeti Kiválóság Program – Hazai hallgatói, illetve kutatói személyi támogatást biztosító rendszer kidolgozása és működtetése országos program című kiemelt projekt keretében zajlott. A projekt az Európai Unió támogatásával, az Európai Szociális Alap társfinanszírozásával valósult meg.



A kutatás a TÁMOP-4.2.2.A-11/1/KONV-2012-0043 számú ENVIKUT projekt keretében, az Európai Unió támogatásával, az Európai Szociális Alap társfinanszírozásával valósult meg.



